ATE HEFAT 2021

15th International Conference Applied Thermal Engineering

Heat Transfer Fluid Mechanics and Thermodynamics

Applied Thermal Engineering

VIRTUAL CONFERENCE

26-28 July 2021

PROCEEDINGS

15th International Conference on Heat Transfer, Fluid Mechanics and Thermodynamics

ASTFE
American Society of Thermal and Fluids Engineers

ICHMT

ENHANCEMENT OF DUAL PHASE PULSATING HEAT PIPES USING HYBRID FERRITIC NANOFLUID UNDER ACTIVE MAGNETIC FIELD

Md. Akib Khan
Department of Mechanical Engineering
Bangladesh University of
Engineering and Technology
Dhaka, 1100
Bangladesh
E-mail: akibkhan035@gmail.com

Dr. AKM Monjur Morshed
Department of Mechanical Engineering
Bangladesh University of
Engineering and Technology
Dhaka, 1100
Bangladesh
E-mail: monjur_morshed@me.buet.ac.bd

Dr. Titan C. Paul
Department of Mathematical
Science & Engineering
University of South Carolina Aiken
SC, 29801
United States
E-mail: titanp@usca.edu

ABSTRACT

Despite being ergonomic heat exchanging devices, used extensively in electronics cooling due to their portability and fast response time, the performance of Heat Pipes are severely obstructed by limitations imposed by the working fluid's thermo-fluid properties. Heat transfer characteristics and cooling time of such a Pulsating Heat Pipe filled with Ferrofluid under magnetic field has been investigated in this computational study using CFD-CHT simulations based on Finite Volume Method implemented by AnSys FLUENT with the MHD module add-on to transcend the aforementioned limitations. Heat transfer and cooling time under realistic thermal loading condition was analyzed with and without presence of magnetic field and the results were compared with that of conventional water loaded ones. With ferrofluid application, increased heat transfer and faster evaporation onset was observed and the performance improved furthermore when external magnetic excitation was applied. As indicated by the simulation, cooling time was also significantly reduced with ferrofluid.

INTRODUCTION

Pulsating heat pipes are passive heat transfer devices that cool objects, mostly hot electronic components that require fast cooling under fluctuating load,by transferring the heat to a working fluid by convective process, which can be both single or multiphase, in a pulsating manner. These devices are essential to get the maximum effectiveness of electronic devices as the performance of electronic components decline exponentially with incremental heat accumulation. Development of a high performance heat pipe will improve usability of electronic devices. But unfortunately there is a limit to this performance enhancement due to low thermal conductivity of available working fluids. This limit however can be transcended if nanofluids are utilized.

Nanofluids are colloidal suspension of nanoscale particulates or structures(nanotubes,nanosheets or nanofibers) in a base fluid. Due to the presence of condensed nanomaterials,thermophysical properties of the base fluid such as convective heat transfer coefficient,diffusivity, specific heat and thermal conductivity

NOMENCLATURE

ρ	$[kgm^{-3}]$	density
ϕ	[-]	volume concentration of nanoparticle in the ferrofluid
C_p	$[Jkg^{-1}K^{-1}]$	specific heat capacity
μ	[Pa·s]	dynamic viscosity
k	$[Wm^{-1}K^{-1}]$	thermal conductivity
n	[-]	shape factor
P	[m]	perimeter of nanoparticle boundary
A	$[m^2]$	surface area of nanoparticle
h	$[Wm^{-2}K^{-1}]$	convection heat transfer co-eff.

Subscripts

nf	nanofluid
np	nanoparticle
bf	bulk fluid

of the overall coloidal system increases significantly. This enhanced characteristics makes them an ideal choice as working fluid for many heat transfer equipment including heat pipe. Using nanofluids as working fluid in heat pipes, independent of the operation type, increment in the performance beyond the capability of ordinary fluid can be achieved. Although there are still problems. Most prominent problem is that the fluid flow faces high drag due to enhanced vortex creation by the moving nanoparticles. Also agglomeration of nanoparticles during evaporation results in segregation of the fluid mix.

Magnetic effects could be used to transcend the limits further. If the nanoparticles suspended in the nanofluid are magnetically responsive, their motion can be controlled via application of active magnetic field. Schliomis et al. [1] demonstrated that such a setup can achieve negative viscosity, that is instead of dragging the flow down the continual shearing of the fluid boosts the flow. This increased mobility adds up to the overall heat transfer coefficient by increasing the associated Reynold's number and the thermal performance is improved much more by thermal conductivity improvement due to microscale induction chaining as reported by Shahsavar et al. [2].

Multiphase application of nanofluids creates some problematic issues regarding stability of the nanofluid. For example deposition of nanoparticles occur at corners and wicked structure can't be used as it interferes with the flow streamline.

In recent years the idea of using nanofluids for heat pipe performance enhancement has been investigated by many researchers. Hussain et al. [3] and Mousavi et al. [4] reported improved cooling response by ferrofluids in constricted channels. Ghofrani et al. [5] demonstrated ferrofluid cooling performance improvement under alternating magnetic fields. This idea of magnetic field coupling is something that deserves more attention as it could be the key factor for creating next generation heat pipes. This is the major driving potential for the current work.

SIMULATION DESIGN

To simulate effect of fluid property variation only, the same heat pipe model is used in all simulations. The model dimensions are chosen based on Antec A400 heat pipe [6] as it is a popular model fabricated using the most recent design for heat pipes. Modifications have been made to the aforementioned dimension to adapt it as a PHP and meet ferrofluid application conditions.

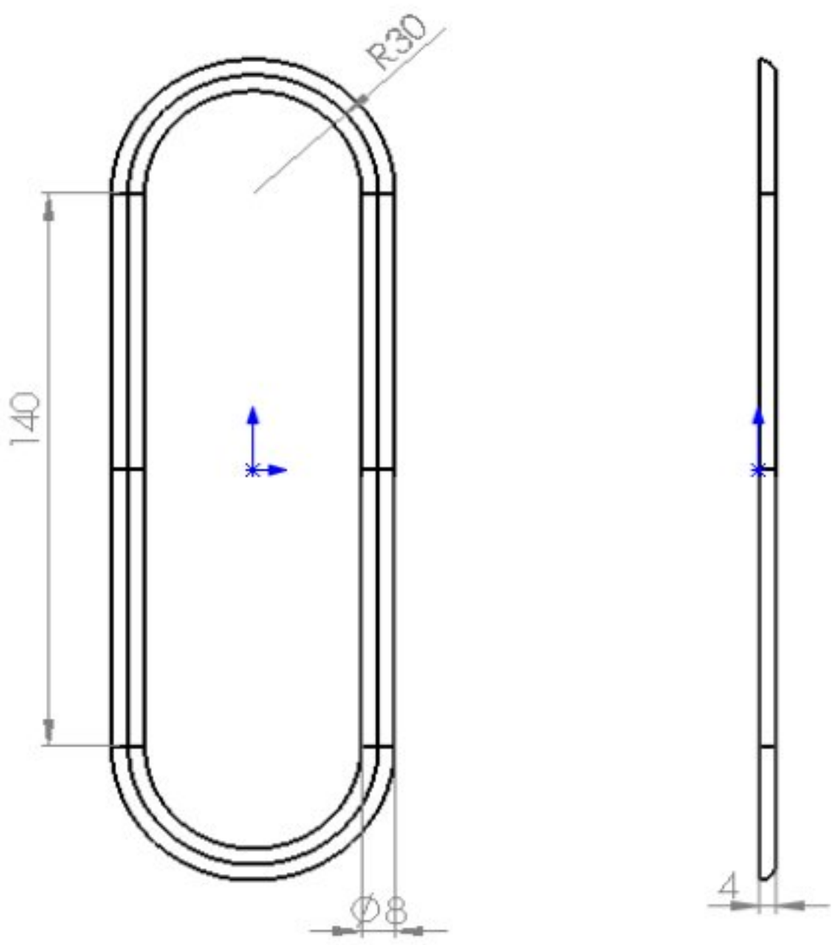

Figure 1. Orthographic projection sketch of model

The World Coordinate System (WCS) was set up with the geometric centroid as origin and *y-axis* pointing from evaporator to condenser to simulate worst case scenario.

The model has been made as a symmetric half-section to permit observational provision to the central plane for monitoring the thermal and phase transition progression during the simulation. Contrary to most regular PHPs only a single loop is considered to reduce computational complexity.

Like all heat pipes three distinct zones for evaporator, adiabatic conductor and condenser have been created. The condenser portion is made significantly larger than evaporator to facilitate condensation as pointed out by Silverstein[7].

NAME OF ZONE	LENGTH SPAN	PROPORTION
Evaporator	30 mm	15%
Adiabatic Conductor	70 mm	35%
Condenser	100 mm	50%
Total	200 mm	100%

Table 1. Zone Proportions in the Model

An additional zone was marked up as symmetry zone to facilitate application of boundary condition and reduce computation time.

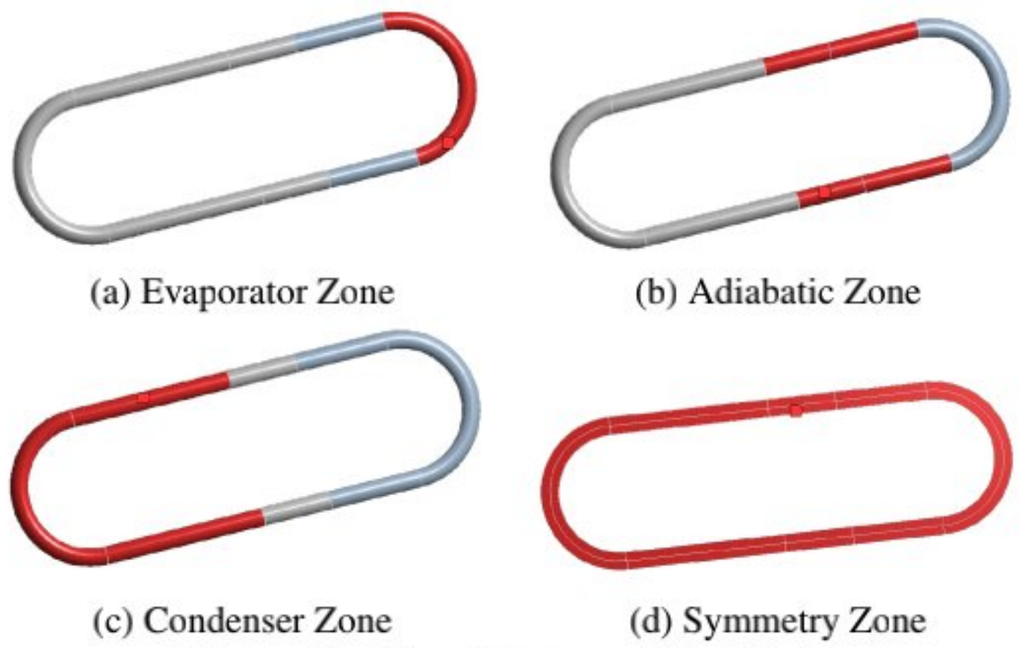

(a) Evaporator Zone (b) Adiabatic Zone

(c) Condenser Zone (d) Symmetry Zone

Figure 2. Zone Markup of the Model

Filling ratio is crucial to heat pipe performance. As reported by Thrayil et al. [8] and Shi et al. [9] too high of a filling ratio hinders completion of proper condensation and too low one creates extended void retention which stalls the cycle.

In accordance with these results an optimum fill ratio of 35% was chosen for the simulation. The air over the working fluid was set up in vacuum pressure levels to permit low temperature vaporization and match the thermal loading scenario.

Walls of the heat pipe are not packed with sintered wick or any type of grooves as these structures interfere with particle lumps formed during evaporation of the ferrofluid. The absence of such capillary boosters is more than mitigated by the pulsating flow mechanism of the PHP, rendering need of such structures obsolete.

Domain Meshing

The mesh for this problem has high dependency on cell size rather than cell shape. Considering optimum time-steps investigated in the works of Ma et al. [10] a cell size of 1.5976×10^{-5} order was chosen. The size couldn't be reduced furthermore due to unavailability of sufficient computational power.

Shape of the cells are tetrahedral with adaptive sizing throughout. The relevance center was set at fine mesh conditions and inflation adjustment has been done. Some cells in the symmetry face have been base flattened to facilitate application of symmetry boundary condition.

Figure 3. Meshing used for the simulation

The mesh is of hybrid nature . More mesh density is provided in the evaporator and condenser sections compared to other zones to make the discretization superior and obtain more reliable thermal data in these principle heat exchanging regions.

Boundary and Initial Conditions

The evaporator was set to receive a positive heat flux of value $5572 W m^{-2}$ in accordance with the TDP(Thermal Design Power) of most common CPUs. A continuous heat flux would make the temperature variation rate slower and hence would take large number of time-steps to observe. To eradicate this problem a pulse of heat flux was applied for a finite amount of time which acts as the thermal load.

Adiabatic section was kept insulated and thermal symmetry was considered for the symmetry zone.

To condense the void flashed on evaporator an approximate isoflux condition to simulate effects of ID fan cooling on the condenser side is set up. The flux value was set to be $342 W m^{-2}$,which is calculated from fan data,with a negative sign to indicate heat removal.

The complete 3D domain was essentially separated in two phases at the beginning, the working fluid liquid phase and air phase. Working fluid vapor would be produced once thermal loading is activated and therefore at the beginning the vapor should be absent in all domains.

The applied magnetic field was chosen to be $10 mT$ so as to obtain magnetic saturation of the working fluid which has LiTi Ferrite(α and γ variants) nanoparticles suspended in a carrier fluid of Acetone and Buckwheat Oil Blend.

RESEARCH METHODOLOGY

The simulation was performed using FVM(Finite Volume Method) with the commercial software Ansys© Fluent. VOF(Volume of Fluid) mixture model was used to represent interaction of the working fluid phases. Three Eulerian phases were assigned as VOF mixture species which were set as primary and secondary phases. Air was set as the primary species to make volume fraction calculations simpler and the two secondary phases are assigned by liquid and vapor phases of the working fluid.

Evaporation-condensation type of mass transfer from working fluid's liquid phase to vapor phase and vice-versa was set as the only mass transfer mechanism. Lee model was used to model the process and saturation temperature of the fluid was set as 333.15 K(60°C) to enable vaporization at the working temperature. The condensation frequency was set higher than the evaporation frequency to account for the slow pace of condensation process. Despite the flow being laminar,k-ε viscosity model with curvature correction and enhanced wall treatment was used to model the viscosity, to obtain data about possible MHD(Magneto Hydro Dynamic) effects.

Properties of the nanofluid are calculated based on proven and validated correlations mentioned below.

Mass Balance :

$$\rho_{nf} = \phi\rho_{np} + (1-\phi)\rho_{bf} \tag{1}$$

Weighted Energy Balance(Eastman et al.[11]):

$$C_{nf} = \frac{\phi\rho_{np}(C_p)_{np} + (1-\phi)\rho_{bf}(C_p)_{bf}}{\rho_{nf}} \tag{2}$$

Tuned Vicosity Model(Maiga et al.[12]):

$$\mu_{nf} = \mu_{bf}(1 - 0.19\phi + 3.6\phi^2) \tag{3}$$

Hamilton-Crosser Model[13]:

$$k_{nf} = k_{bf}\frac{k_{np} + (n-1)k_{bf} - (n-1)(k_{bf} + k_{np})\phi}{k_{np} + (n-1)k_{bf} + (k_{bf} + k_{np})\phi} \tag{4}$$

$$n = \frac{P}{\sqrt{A}}$$

To monitor vapor generation from the very beginning and observe complete cycle in multiple frames the time step is set in the order of 3×10^{-5} and the time-step iterations are run in groups of 1000.

To simulate the case where external magnetic field is present an additional package with identifier MHD Module was activated. This module was used to setup magnetic properties of the working fluid, specify proper magnetic-coupling models and calculate additional parameters by solving Maxwell equations in addition to the conventional CFD equations(*i.e.* Navier-Stokes).

Before solver is run proper time-step is to be selected to ensure convergence. Although the CFL(Courant-Friedrich-Levy) number gives a guideline, this selection is mostly trial and error.

Also the under relaxation factor for energy parameter should be decreased to adapt with the large variations in energy during the thermal loading application period. It is generally set as unity but should be tweaked until convergence is found. For the current work a value of 0.7 was found to be suitable.

Validation of Generated Mesh

To validate the generated mesh, two different meshing constructs are used to generate two different meshing setups with distinct cell sizes which are run through simulation under similar test condition to generate a thermal behavior plot.

Data obtained from the two meshing configurations was then used to generate Nusselt Number (Nu) versus Reynold's Number (Re) graph representing heat transfer characteristics of the heat pipe in these two cases. Data for these parameters were taken at the evaporator section as the significant portion of heat transfer occurs in this section. The two curves were plotted against each other and similarity trend was investigated.

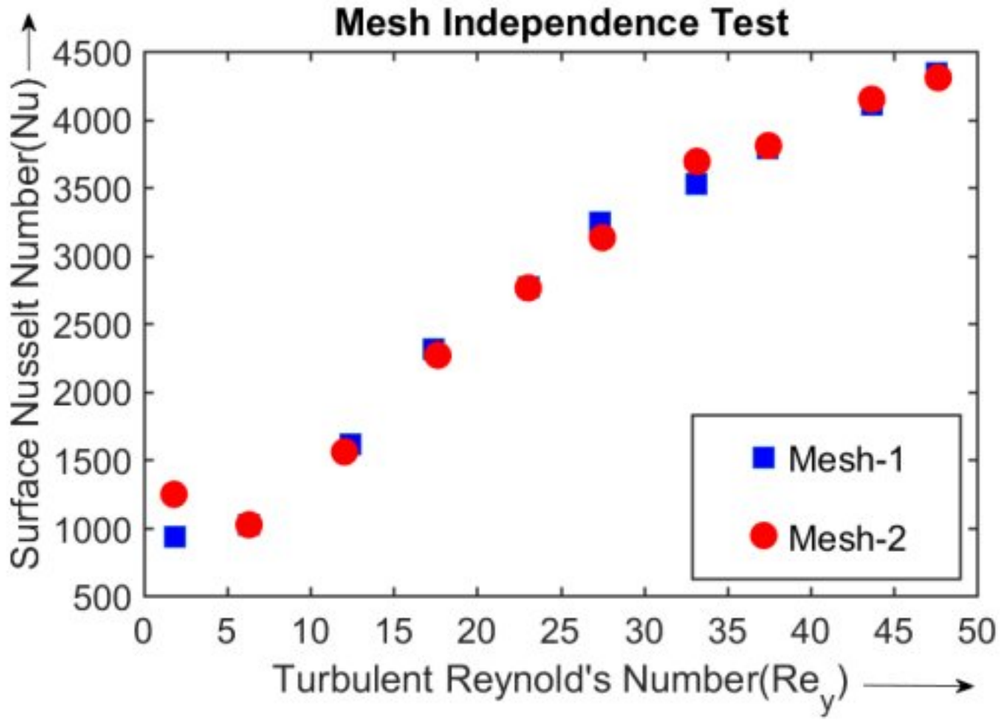

Figure 4. Nu vs. Re plot in evaporator section for two distinct mesh constructs

In *figure 4*, the curves show near perfect match(maximum deviation of 4.7 %) which suggests mesh independence has been established. The deviation between the two data is exceptionally high at very low Re. This is due to the fact that at very low Re values the velocity field is unstable due to excess viscous drag.

The thermal behavior observed in *figure 4* is also in agreement with the works of Ghofrani et al. [5]. This agreement validates the results of this study.

Post-processing of Results

To observe cooling effect and vapor generation, contour plots of total temperature and vapor volume fraction are generated in all domains. The contour plots served as the principal visualization tool for this study to concisely summarize the results. These contours can easily be animated using time-step animation generator. This initial post processing was done in CFD Post®.

To generate time evolution or two parameter correlation curves a probe point is to be selected where the parameter variation data would be collected from. Two probe points located at (0,-0.1,-0.002) and (0,0.1,-0.002) were considered as representatives of evaporator and condenser section. The data was filtered using regression strategy to exclude potential outliers. The data processing steps are performed using MS Excel®. The final plotting is done using Matlab®.

RESULTS AND COMPARISON

To observe cooling performance of the heat pipe, temperature variation with time is observed. Also to quantify the thermal load, heat transfer behavior(Nu vs re) is monitored. Finally to identify magnetic field effect on the phase transition process, contours of void propagation are generated.

Cooling Curves

The evaporator cooling with nanofluid is found to be higher than that of conventional ones that use water. In *figure 5* the curve for nanofluid shows an approximately exponential trend which suggests the system is of first order nature, whereas the curve for water is mostly linear.

When the magnetic field is activated, initially the performance is found to be lower but eventually after a cut-point magnetohydrodynamic effects become significant and the cooling becomes faster. The inflection that the nanofluid curve experiences at cut-point is due to agglomeration of nanoparticles during vapor generation. The inflection is absent in case of water due to null agglomeration.

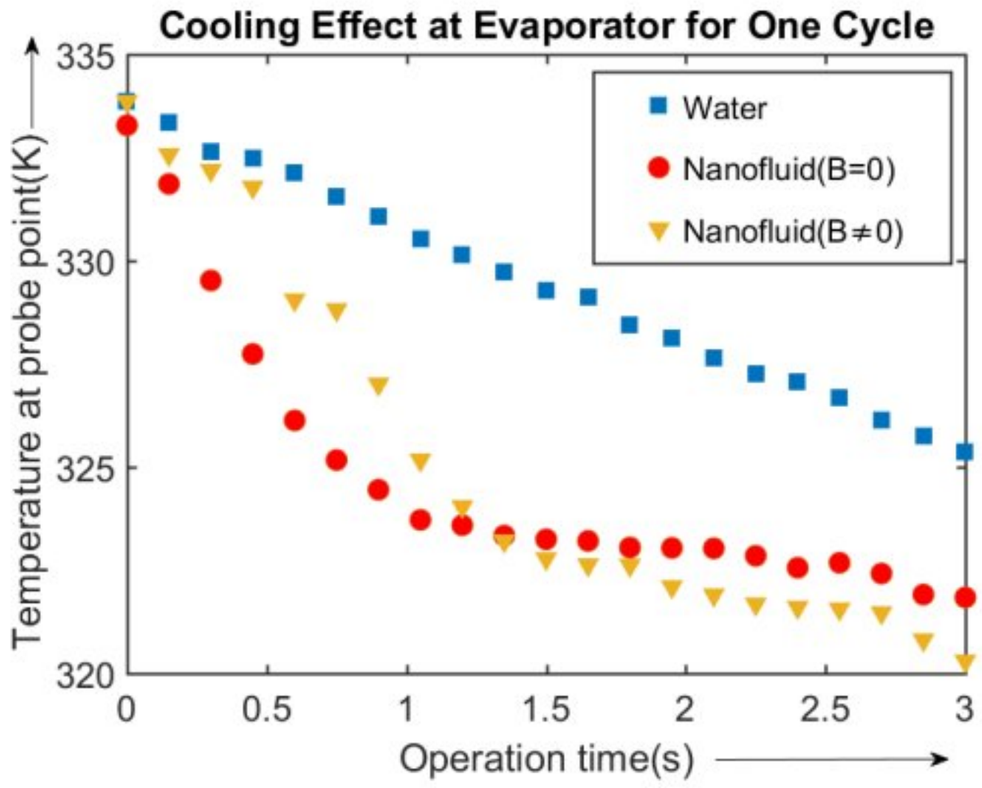

Figure 5. Evaporator cooling behavior comparison

The lower performance in the beginning, as observed in *figure 5*, is due to strong opposing magnetic induction in the ferrofluid due to Lenz's law of induction. The fluid flowfield undergoes a complex microscopic assortment, eventually reaching a cut point. The additional pressure gradient created during this phase provides advective acceleration to the fluid once this point is passed which elevates the performance after this cut-point.

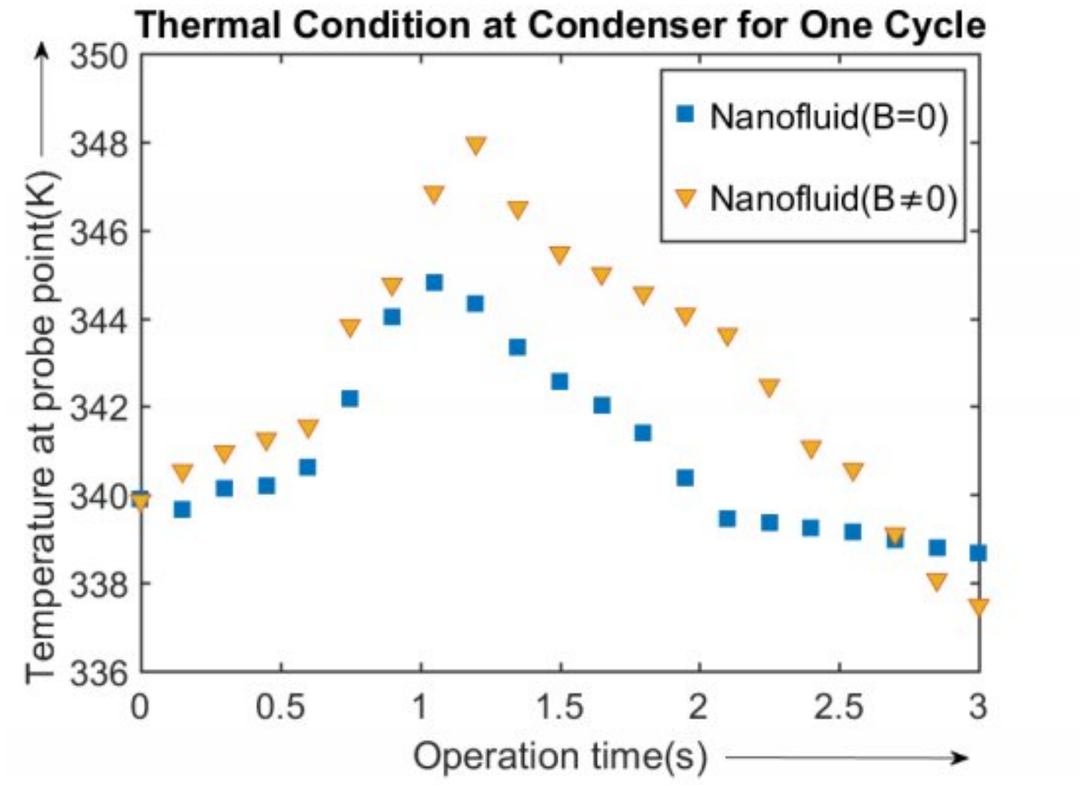

Figure 6. Condenser temperature variation comparison

Due to different amount of heat flux absorption at the evaporator in different working conditions, the heat rejection and hence temperature levels at the condenser are different as indicated in *figure 6*.

As ferrofluid picks up more heat compared to nanofluid (as shown in *figure 5*) at the evaporator, it rejects more heat at the condenser resulting in higher levels of peak temperature at the condenser. The higher heat pick-up would ultimately prove to be beneficial in the long run as it would cool the target heat source faster providing a shorter overall response time.

Heat Transfer

To compare heat transfer behavior of the heat pipe, Nu versus Re plots have been observed as demonstrated in *figure 7*. With presence of magnetic field, the values of 'h' are higher due to: velocity boost resulting from thermomagnetic pumping[14], thermal conductivity increment due to anisotropy reduction, higher evaporation frequency due to multi-nucleation.

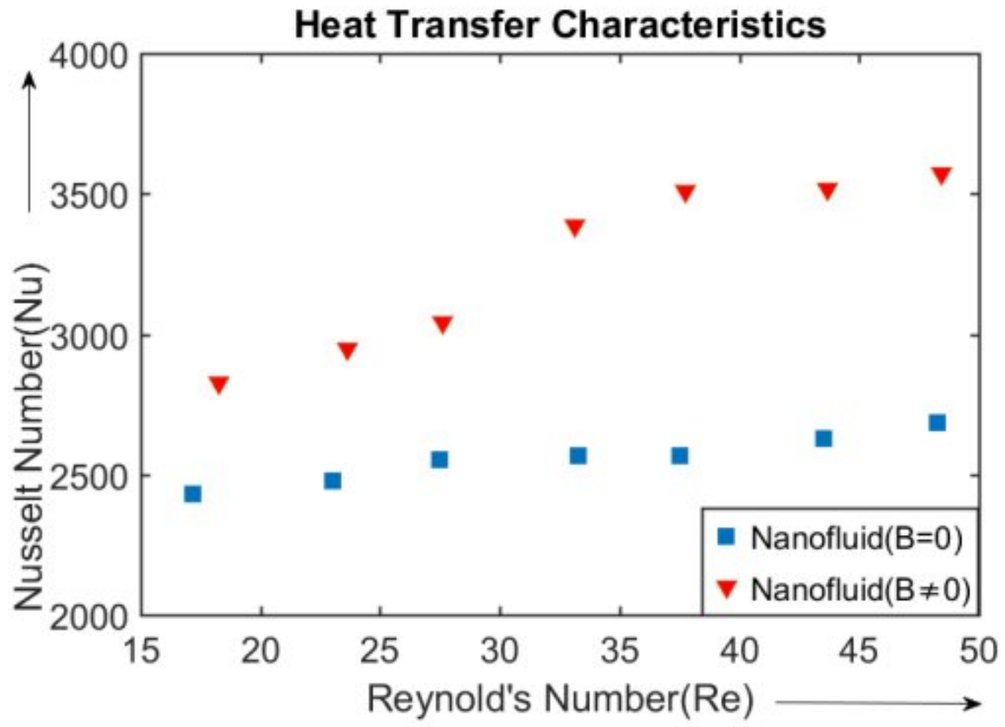

Figure 7. Heat transfer comparison

The gap between active and inactive magnetic excitation increases with increasing Re due to additional vortex formation and magnetohydrodynamic turbulence which increases 'h' and hence the heat transfer.

Vapor Progression

The vaporization pattern is observed by generating time-step animation based on contour plots of the vapor volume fraction. These demonstrate progression of voids generated during evaporation through the working fluid. The lumped mass dynamics visualizes the mass transfer during phase-change and demonstrates magnetic field effect on the phase transition process.

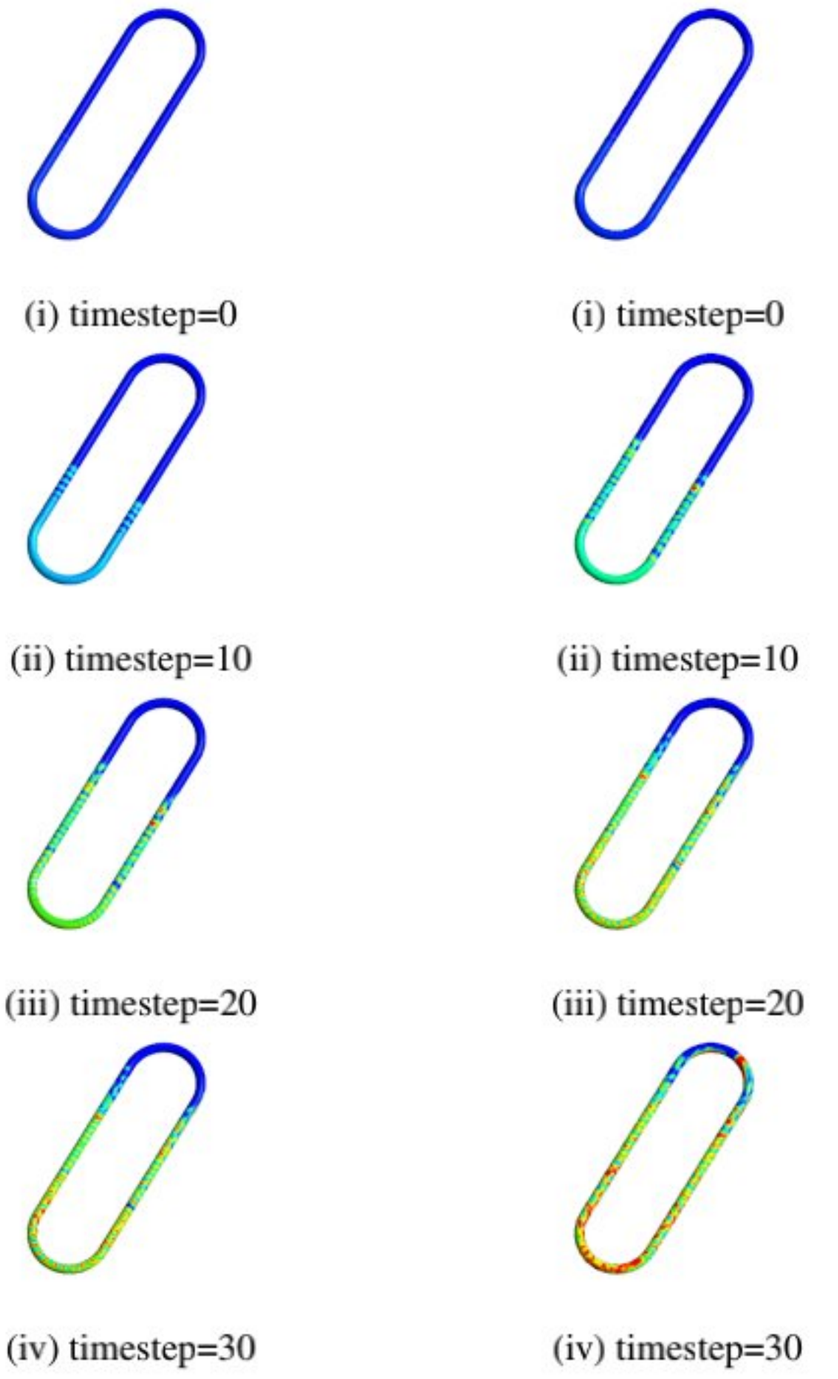

Figure 8. Comparison of vapor evolution

As it can be seen from time-frames of contour plot in *figure 8*, the vapor progresses symmetrically through both parallel pipe segments when no magnetic field is present but the progression is asymmetric under magnetic field. The vapor propagation process is accelerated once the magnetic field speeds up the fluid. Eventually the two vapor streams collide at the condenser reducing bulk motion and facilitating the condensation process. This makes condensation start faster under magnetic excitation.

CONCLUSION

In this computational study thermo-fluid performance of ferrofluid is investigated by observing heat transfer,overall cooling

speed and flow characteristics. The results are summarized as follows-

- *Heat Removal Rate* of the heat pipe is found to be higher under the presence of magnetic field.
- *Vapor Onset* is quicker and more nucleation site formation occurs when magnetic field is present.
- *Void Spread* in the magnetically excited ferrofluid is faster due to quicker vapor onset.
- *Velocity Field* under magnetic excitation is more vigorous which makes Re values much higher.
- *Response Speed* is initially lower due to opposing magnetic induction,as suggested by Lenz's law, but quickly increases once thermomagnetic pumping effects become prominent. This increases the overall response speed drastically.

REFERENCES

[1] Mark I. Shliomis and Konstantin I. Morozov. Negative viscosity of ferrofluid under alternating magnetic field. *Physics of Fluids*, 6(8):2855–2861, August 1994.

[2] Amin Shahsavar, Mohammad Reza Salimpour, Mohsen Saghafian, and M. B. Shafii. Effect of magnetic field on thermal conductivity and viscosity of a magnetic nanofluid loaded with carbon nanotubes. *Journal of Mechanical Science and Technology*, 30(2):809–815, February 2016.

[3] Mohammed Noorul Hussain and Isam Janajreh. Numerical simulation of a cylindrical heat pipe and performance study. *International Jouranl of Thermal & Environmental Engineering*, 12(2):135–141, 2016.

[4] S. Valiallah Mousavi, M. Barzegar Gerdroodbary, Mohsen Sheikholeslami, and D. D. Ganji. The influence of a magnetic field on the heat transfer of a magnetic nanofluid in a sinusoidal channel. *The European Physical Journal Plus*, 131(9), September 2016.

[5] Ali Ghofrani, M.H. Dibaei, Abbas Hakim sima, and Mohammad Shafii. Experimental investigation on laminar forced convection heat transfer of ferrofluids under an alternating magnetic field. *Experimental Thermal and Fluid Science*, 49:193–200, 09 2013.

[6] *Antec A400 Heat Pipe*. Available at https://antec.com/product/cooling/a400-rgb.php.

[7] C C Silverstein. *Design and Technology of Heat Pipes for Cooling and Heat Exchange*. United States, 1st edition edition, 1992.

[8] Trijo Tharayil, Lazarus Godson Asirvatham, Vysakh Ravindran, and Somchai Wongwises. Effect of filling ratio on the performance of a novel miniature loop heat pipe having different diameter transport lines. *Applied Thermal Engineering*, 106:588–600, August 2016.

[9] Weixiu Shi and Lisheng Pan. Influence of filling ratio and working fluid thermal properties on starting up and heat transferring performance of closed loop plate oscillating heat pipe with parallel channels. *Journal of Thermal Science*, 26(1):73–81, January 2017.

[10] H. B. Ma, M. A. Hanlon, and C. L. Chen. An investigation of oscillating motions in a miniature pulsating heat pipe. *Microfluidics and Nanofluidics*, 2(2):171–179, December 2005.

[11] J.A. Eastman, S.R. Phillpot, S.U.S. Choi, and P. Keblinski. Thermal transport in nanofluids. *Annual Review of Materials Research*, 34(1):219–246, 2004.

[12] Sidi Maïga, Samy Palm, Cong Nguyen, Gilles Roy, and Nicolas Galanis. Heat transfer enhancement by using nanofluids in forced convection flows. *International Journal of Heat and Fluid Flow,Elsevier(SCOPUS Indexed)*, 26:530–546, 08 2005.

[13] R. L. Hamilton and O. K. Crosser. Thermal conductivity of heterogeneous two-component systems. *Industrial & Engineering Chemistry Fundamentals*, 1(3):187–191, August 1962.

[14] H.O.G. Alfven. Cosmology in the plasma universe: an introductory exposition. *IEEE Transactions on Plasma Science*, 18(1):5–10, 1990.